Electrical characterization of high k-dielectrics for 4H-SiC MIS devices

Citation for the original published paper (version of record):

Khosa, R., Chen, J., Winters, M. et al (2019)
Electrical characterization of high k-dielectrics for 4H-SiC MIS devices
Materials Science in Semiconductor Processing, 98: 55-58
http://dx.doi.org/10.1016/j.mssp.2019.03.025

Materials Science in Semiconductor Processing 98 (2019) 55–58

Contents lists available at ScienceDirect

Materials Science in Semiconductor Processing

journal homepage: www.elsevier.com/locate/mssp

Electrical characterization of high k-dielectrics for 4H-SiC MIS devices

R.Y. Khosa[a,b,*], J.T. Chen[c], M. Winters[d], K. Pálsson[a], R. Karhu[c], J. Hassan[c], N. Rorsman[d], E.Ö. Sveinbjörnsson[a,c]

[a] Science Institute, University of Iceland, Iceland
[b] Department of Physics, University of Education Lahore, Dera Ghazi Khan Campus, 32200, Dera Ghazi Khan, Pakistan
[c] Department of Physics, Chemistry and Biology (IFM), Semiconductor Materials Division, Linköping University, SE-58183, Linköping, Sweden
[d] Department of Microtechnology and Nanoscience, Chalmers University of Technology, SE-41296, Göteborg, Sweden

ARTICLE INFO

Keywords:
Interface traps
AlN/4H-SiC interface
Al_2O_3/4H-SiC interface
MIS structure

ABSTRACT

We report promising results regarding the possible use of AlN or Al_2O_3 as a gate dielectric in 4H-SiC MISFETs. The crystalline AlN films are grown by hot wall metal organic chemical vapor deposition (MOCVD) at 1100 °C. The amorphous Al_2O_3 films are grown by repeated deposition and subsequent low temperature (200 °C) oxidation of thin Al layers using a hot plate. Our investigation shows a very low density of interface traps at the AlN/4H-SiC and the Al_2O_3/4H-SiC interface estimated from capacitance-voltage (CV) analysis of MIS capacitors. Current-voltage (IV) analysis shows that the breakdown electric field across the AlN or Al_2O_3 is ~ 3 MV/cm or ~ 5 MV/cm respectively. By depositing an additional SiO_2 layer by plasma enhanced chemical vapor deposition at 300 °C on top of the AlN or Al_2O_3 layers, it is possible to increase the breakdown voltage of the MIS capacitors significantly without having pronounced impact on the quality of the AlN/SiC or Al_2O_3/SiC interfaces.

1. Introduction

The great potential of 4H-SiC MISFETs for power electronics is hampered by low channel mobility mainly due to high density of interface states at the SiO_2/SiC interface. The quality of the SiO_2/SiC interface has been improved by various oxidation and nitridation methods but more reduction in interface traps is needed [1–3]. Beside SiO_2 as a gate dielectric, the use of high-k dielectrics on SiC has also been investigated. AlN and Al_2O_3 have reasonably large band gap (~ 6.2 eV and ~7 eV respectively) and high dielectric constant. The conduction band offset of AlN or Al_2O_3 to 4H-SiC of ~ 1.7 eV is expected to be sufficient for n-channel MISFET operation [4–9]. High quality single crystalline AlN can be grown on SiC because of only 1% lattice mismatch to SiC [10]. However, an amorphous Al_2O_3 is considered to be better than poly-crystalline α-Al_2O_3 as a gate dielectric on 4H-SiC because of leakage through grain boundaries [11].

A crystalline AlN grown by molecular beam epitaxy (MBE) has been reported as a gate dielectric for 4H-SiC MISFETs but very low channel mobility (< 1 cm^2/V) was obtained because of the leaky structure [12]. The irradiation of atomic nitrogen or HCl gas etching before the growth of AlN has been used to improve the quality of MBE grown AlN films [13,14]. The growth of AlN layers by MOCVD on 4H- and 6H-SiC has also been reported and a significant density of fixed charge and interface traps is observed in such AlN layers [15,16].

An amorphous Al_2O_3 grown by atomic layer deposition (ALD) or thermal oxidation of metallic Al has been used as a gate dielectric in graphene field effect transistors with some success [17,18]. The ALD as grown Al_2O_3 on 4H-SiC typically contains a large number density of negative charges which are reduced after annealing in Ar at 1000 °C but the Al_2O_3/SiC interface contains a high density of interface traps after such treatment due to growth of an interfacial SiO_x ($0 < x < 2$) layer [19]. To improve the quality of ALD grown Al_2O_3, pre-deposition surface cleaning and post deposition annealing has been performed in N_2O or N_2 ambient [20,21]. A MOSFET with ALD grown Al_2O_3, that was post-annealed in hydrogen at 400 °C, is reported with a field effect mobility of 57 cm^2/V. Even though these results are promising, large threshold voltage shifts are observed due to the sensitivity of the Al_2O_3 layers to electron injection [22]. There is another report on a very high peak field effect mobility of 300 cm^2/V in SiC MOSFETs using Al_2O_3 made by MOCVD with a thin SiO_2 interfacial layer to the SiC [23]. But, the mobility drops very rapidly with gate voltage and is less than 50 cm^2/V at moderate gate voltages.

* Corresponding author. Science Institute, University of Iceland, Iceland.
E-mail addresses: ryk2@hi.is (R.Y. Khosa), jrche@ifm.liu.se (J.T. Chen), micwinte@chalmers.se (M. Winters), kjp9@hi.is (K. Pálsson), robka36@ifm.liu.se (R. Karhu), jawul@ifm.liu.se (J. Hassan), niklas.rorsman@chalmers.se (N. Rorsman), einars@hi.is (E.Ö. Sveinbjörnsson).

https://doi.org/10.1016/j.mssp.2019.03.025
Received 5 September 2018; Received in revised form 7 February 2019; Accepted 20 March 2019
Available online 28 March 2019

In this study, we grow crystalline AlN by hot wall MOCVD and amorphous Al_2O_3 by low temperature oxidation of Al on n-type 4H-SiC. On few selected samples, an additional layer of SiO_2 is deposited on top of the AlN or Al_2O_3 layer by plasma enhanced chemical vapor deposition (PECVD). The interface traps at the AlN/SiC and Al_2O_3/SiC interfaces are investigated by capacitance voltage (CV) measurements on MIS capacitors. The dielectric breakdown properties are extracted from current voltage (IV) measurements. We find that both the AlN/SiC and the Al_2O_3/SiC interface contain very low density of interface traps and the use of SiO_2/AlN or SiO_2/Al_2O_3 dielectric stack improves the breakdown voltage of the MIS devices.

2. Experimental methods

Two sets of n-type 4H-SiC MIS capacitors were made. One with single crystalline AlN and other with amorphous Al_2O_3 as a dielectric. The 4H-SiC used in this study have 10 μm thick n-type epitaxial layers with a net doping concentration of $\sim 1 \times 10^{16}$ cm^{-3} grown on 4° off-axis (0001) highly doped $\sim 1 \times 10^{18}$ cm^{-3} 4H-SiC substrates. A single crystalline 10 nm thick AlN layer was grown on 4H-SiC in a horizontal hot-wall MOCVD reactor at 1100 °C. Ammonia and $Al_2(CH_3)_6$ were used as a precursor for nitrogen and aluminum respectively. Prior to deposition of AlN, the SiC surface was exposed in H_2 ambient at 1320 °C, in order to obtain a native oxide-free surface. The details of the AlN growth process and structural characterization of the crystalline AlN layers are given in Ref. [24]. The amorphous Al_2O_3 is grown by depositing few monolayers of pure Al by electron beam evaporation at a rate of $\sim$ 0.5 Å/s and then the sample is baked on a hot plate in room environment at a temperature of 200 °C for 5 min to form Al_2O_3 layer. This process of deposition and subsequent low temperature oxidation was repeated twelve times resulting in a film thickness of 15 nm as determined by X-ray reflectivity (XRR) and Atomic Force Microscopy. Prior to growth of Al_2O_3, the SiC was cleaned with HF in order to remove the native oxide. Further details of the Al_2O_3 growth process are given in Ref. [25]. An additional layer of SiO_2 with thickness of 40 nm was deposited on selected samples from both sets by PECVD at 300 °C using source gases of nitrous oxide and silane. Reference MIS capacitors with thermal SiO_2 grown in dry oxygen or in N_2O ambient were also analyzed. Samples with identical reference oxides have previously been used in SiC MOSFETs [26]. The dielectric thickness of all samples was estimated using X-ray reflectivity (XRR) and the crystallinity was investigated with X-ray diffraction (XRD). Our Al_2O_3 and SiO_2 films are amorphous, no crystallization is observed by XRD apart from the AlN samples [24].

Circular MIS capacitors are made using Al as a gate metal and back contact as well. The interface quality is characterized by conventional CV analysis using Agilent E4980A LCR meter. The dielectric breakdown strength of the MIS samples is determined by IV measurements using a Keithley 617 electrometer. CV and IV measurements are performed in vacuum of 10^{-3} mbar in a cryostat.

3. Results and discussion

Fig. 1 shows CV spectra of MIS capacitors having AlN and Al_2O_3 dielectrics measured at room temperature and at frequencies of 1 kHz and 1 MHz. The gate bias is swept from depletion (negative bias) to accumulation (positive bias) and the capacitance signal for both frequencies is recorded simultaneously at each gate bias point. Fig. 1a shows the CV curves for AlN sample. The dielectric constant deduced from the accumulation capacitance is about 8.7. Fig. 1b shows the CV spectra of the Al_2O_3. The dielectric constant for Al_2O_3 is $\sim$ 6.5. The flatband voltage in both AlN and Al_2O_3 is $\sim$ 0.7 V which is close to the theoretical flatband voltage (i.e. $\sim$ 0.4 V) which shows that initially the AlN and Al_2O_3 layers contain insignificant amount of fixed charge. A first estimate of the interface trap density is extracted from frequency dispersion of CV curves [27]. In the AlN and Al_2O_3 case, such dispersion is hardly visible indicating a low interface state density.

The interface quality of AlN or Al_2O_3 dielectric with 4H-SiC can be estimated by investigating the frequency dispersion of the CV spectra of an MIS capacitor. Electron capture into interface states is most often a fast process while electron emission from interface traps is normally much slower and is a thermal process which depends on the difference E_c-E (where E is the energy level of the interface trap and E_c denotes the SiC conduction band edge). If an electron is captured and not emitted again, this is detected as a shift of the CV curve to higher gate voltages. If the test frequency is high (1 MHz) then more traps will not emit their electrons and the curve is shifted as compared to the low frequency (1 kHz) curve. The extraction of D_{it} follows the method of Berglund [27]. The interface trap density (D_{it}) is determined by well-known High-Low-Capacitance method using an equation: $D_{it} = \frac{1}{q}\left(\frac{C_d C_{lf}}{C_d - C_{lf}} - \frac{C_d C_{hf}}{C_d - C_{hf}}\right)$. Where C_d is dielectric capacitance, C_{lf} and C_{hf} are low and high frequency capacitance respectively.

Fig. 2 shows D_{it} extracted from room temperature CV dispersion data for MIS samples with AlN or Al_2O_3 as a dielectric as well as reference SiO_2 samples. The single layer AlN and Al_2O_3 samples contain the lowest D_{it}. The detrimental interface states that exist within this energy range for thermally grown oxides are virtually absent at the AlN/SiC or the Al_2O_3/SiC interface. It is clear that the addition of a SiO_2 dielectric layer on the top of AlN or Al_2O_3 affects the AlN/SiC and Al_2O_3/SiC interfaces. However, the single AlN and the SiO_2/AlN stack both have lower D_{it} than reference samples. The D_{it} of the SiO_2/Al_2O_3 stack is comparable to the reference N_2O grown SiO_2.

A sensitivity to electron injection is observed in both AlN and Al_2O_3 samples. This is detected as a flatband shift in subsequent 100 kHz CV curves when the samples are repeatedly biased into accumulation. The magnitude of the shift depends on the maximum applied accumulation voltage. An example of such behavior is shown in Fig. 3 for single layer AlN and Al_2O_3 MIS samples. Such behavior is also reported in literature for AlN and Al_2O_3 MIS samples [14,19]. This flatband shift can be a result of trapping of electrons in defects located within the dielectric. Similar electron injection is also observed in the dielectric stacks (not shown here).

However, in this work the process is reversible since the trapped electrons can be released back to the SiC at room temperature by applying depletion bias stress and UV illumination for a certain time to the MIS capacitors [28–30]. An example of such an experiment is shown in Fig. 4 for AlN/SiO_2 and Al_2O_3/SiO_2 stack samples. In the case of the AlN/SiO_2 sample (Fig. 4a), the MIS capacitor is initially kept in accumulation (+11 V) for 30 min at room temperature and then sequentially the bias with 100 kHz frequency is swept to depletion (−10 V) and the CV is recorded seen as the black solid curve. Electrons are intentionally injected into the AlN layer during the bias stress. Next, a UV light is shined on the sample under depletion bias of −10 V for 30 min to examine if electrons are released from AlN traps. A broken black 100 kHz CV curve is recorded directly thereafter. A stretch-out of the CV curve at gate voltage from -5 V to 7 V suggests that electrons are released from traps during UV exposure, but they are recaptured to traps as the gate voltage leads the device to accumulation. The same procedure is applied to the Al_2O_3/SiO_2 sample with accumulation and depletion bias of +5 V and -5 V respectively (shown in Fig. 4b) and the results are similar to the AlN/SiO_2 sample. This experiment shows that the AlN and Al_2O_3 layers have traps which capture free electrons during accumulation bias stress and re-emission of the captured electrons is made possible by UV illumination. Applying depletion bias in the same manner but without applying UV light results in a negligible shift of the CV curves (not shown).

IV measurements are used to estimate the critical breakdown field of the dielectrics. Fig. 5 compares the dielectric breakdown field of the AlN and Al_2O_3 samples as well as of reference dry SiO_2 sample based on current density measurement as a function of the effective electric field (J-E) across the gate dielectric. A breakdown field of $\sim$ 3 MV/cm (solid

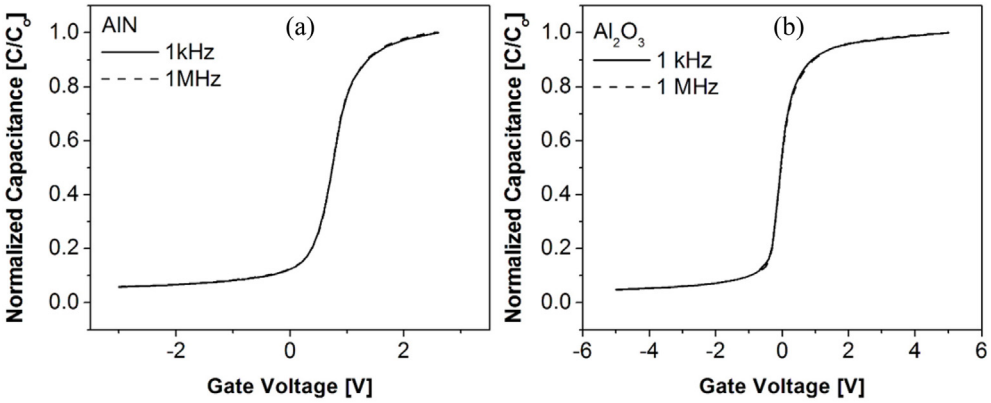

Fig. 1. Room temperature CV curves for (a) AlN and (b) Al_2O_3 samples at test signal frequencies of 1 kHz and 1 MHz.

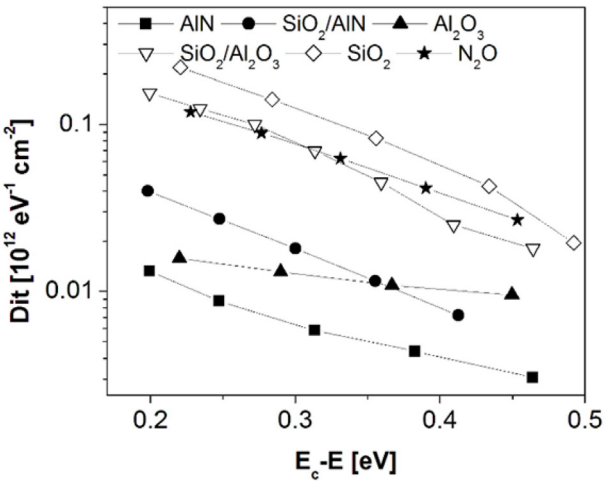

Fig. 2. Comparison of the density of interface states (D_{it}) estimated from CV (at 298 K) as a function of energy for AlN and Al_2O_3 based MIS capacitors along with reference SiO_2 MIS capacitors.

curve) or 5 MV/cm (dotted curve) is recorded for the single layer AlN or Al_2O_3 sample respectively. A sharp current leakage is observed for single layer AlN even at low dielectric electric fields. This suggests the AlN layers have higher density of bulk traps compared to Al_2O_3 that cause trap assisted leakage across dielectric. The breakdown field of the reference thermal SiO_2 sample is ~ 9 MV/cm (dash double dotted curve). The physical origin of the electron traps within the AlN and Al_2O_3 layers is unknown. Our postulate is that the AlN layer has either very high density of intrinsic point defects (e.g silicon and oxygen point defects) or extended defects like dislocations [31]. The Al_2O_3 layer is expected to contain oxygen related intrinsic defects [32]. These defects are presumably the cause of the current leakage through the AlN and Al_2O_3 layers.

The SiO_2/AlN and SiO_2/Al_2O_3 stack samples have effective breakdown field, if we consider the dual dielectric as a single dielectric, of ~ 8 MV/cm (dashed curve for SiO_2/AlN and dash dotted curve for the SiO_2/Al_2O_3 sample). However, the breakdown electric field across the AlN or Al_2O_3 layer in the stack is ~ 4 MV/cm or ~ 5.5 MV/cm. Addition of SiO_2 on the top of AlN layer does not significantly improve the breakdown properties of the AlN or Al_2O_3 but allows the use of higher gate voltages for device operation.

4. Conclusions

CV analysis at room temperature shows that single crystalline AlN and amorphous Al_2O_3 layer have good interface quality in terms of low density of interface states in n-type 4H-SiC MIS capacitors. A significant electron trapping is observed within the AlN or Al_2O_3 when the MIS capacitors are biased into accumulation resulting in a large flatband voltage shift towards higher gate voltages. This can be connected to the relatively low breakdown field (~ 3 MV/cm or ~ 5 MV/cm) of the AlN or Al_2O_3 layers. It is possible to slightly improve the breakdown field of the MIS devices by depositing a SiO_2 layer on top of the AlN or Al_2O_3. More work is needed in optimizing the growth conditions of the dielectrics and resolving the question of electron trapping within the AlN and Al_2O_3 layers. In summary, the AlN and Al_2O_3 MIS samples show very promising results in terms of interface state densities but electron injection into both layers is currently preventing their practical use.

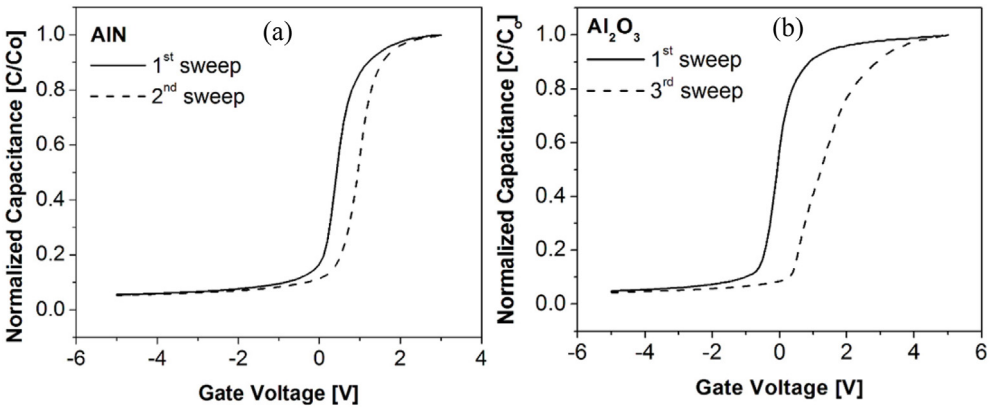

Fig. 3. Subsequent 100 kHz CV sweeps for single layer (a) AlN and (b) Al_2O_3 sample at room temperature.

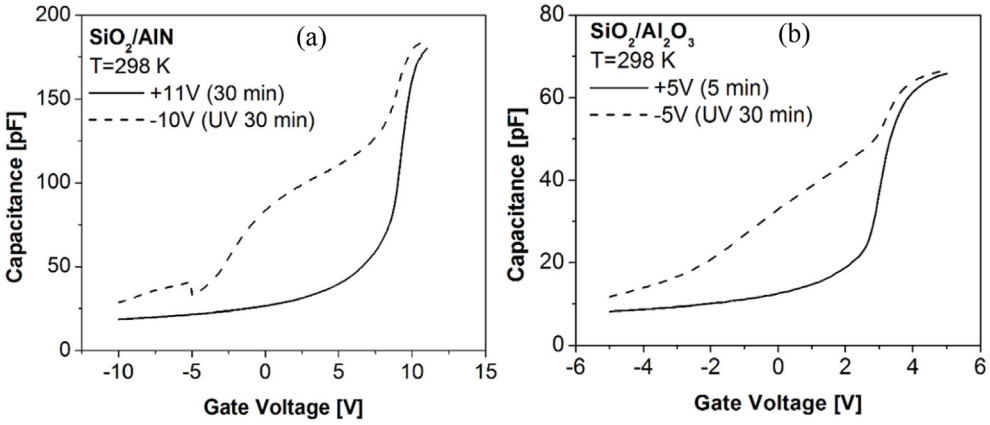

Fig. 4. Electron injection and emission in and out of traps located within (a) the AlN or (b) Al_2O_3 layer. The black solid 100 kHz CV curves are recorded after which electrons are intentionally injected into the AlN or Al_2O_3 by accumulation bias stress for certain period. The dotted 100 kHz CV curves are recorded after applying negative bias stress with UV illumination to the samples for 30 min.

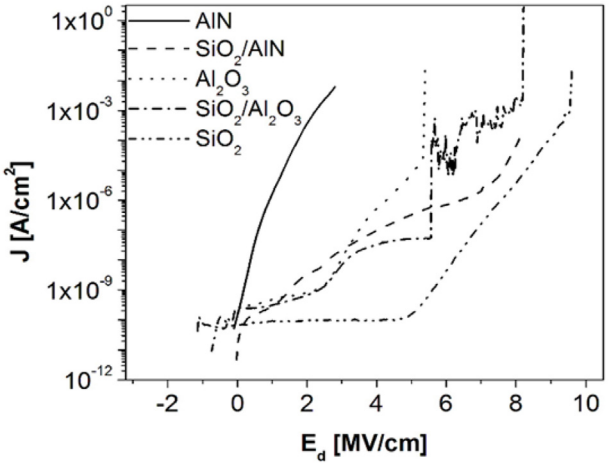

Fig. 5. Comparison of leakage current density versus effective electric field (J–E) for differently prepared MIS samples.

Acknowledgements

This work was financially supported by The Icelandic Research Fund. We also acknowledge support from the Swedish Foundation for Strategic Research (SSF), and the Knut and Alice Wallenberg Foundation (KAW).

References

[1] Y. Jia, H. Lv, Q. Song, X. Tang, L. Xiao, L. Wang, G. Tang, Y. Zhang, Appl. Surf. Sci. 397 (2017) 175.
[2] S.R. Kodigala, S. Chattopadhyay, S. Overton, I. Ardoin, B.J. Gordon, D. Johnstone, D. Roy, D. Barone, Appl. Surf. Sci. 330 (2015) 465.
[3] T. Kimoto, Jpn. J. Appl. Phys. 54 (2015) 040103.
[4] M. Nawaz, Hindawi Publishing Corporation Active and Passive Electronic Components, (2015), p. 1 (2015).
[5] M.O. Aboelfotoh, R.S. Kern, S. Tanaka, R.F. Davis, C.I. Harris, Appl. Phys. Lett. 69 (1996) 2873.
[6] R.D. Vispute, A. Patel, K. Baynes, B. Ming, R.P. Sharma, T. Venkatesan, C.J. Scozzie, A. Lelis, T. Zheleva, K.A. Jones, MRS Online Proc. Libr. 595 (1999) F99W11.3.
[7] J. Choi, R. Puthenkovilakam, J.P. Chang, Appl. Phys. Lett. 86 (2005) 192101.
[8] V.V. Afanasev, F. Ciobanu, S. Dimitrijev, G. Pensl, A. Stesmans, J. Phys. Condens. Matter. 16 (2004) 1839.
[9] F. Zheng, G. Sun, L. Zheng, S. Liu, B. Liu, L. Dong, L. Wang, W. Zhao, X. Liu, G. Yan, L. Tian, Y. Zeng, J. Appl. Phys. 113 (2013) 044112.
[10] K. Wongchotigul, N. Chen, D.P. Zhang, X. Tang, M.G. Spencer, Mater. Lett. 26 (1996) 223.
[11] C.M. Tanner, Y.-C. Perng, C. Frewin, S. Saddow, J.P. Chang, Appl. Phys. Lett. 91 (2007) 203510.
[12] M. Horita, M. Noborio, T. Kimoto, J. Suda, IEEE Trans. Electron Dev. 35 (2014) 339.
[13] N. Onojima, J. Kaido, J. Suda, T. Kimoto, H. Matsunami, Mater. Sci. Forum 457–460 (2004) 1569.
[14] N. Onojima, J. Suda, H. Matsunami, Appl. Phys. Lett. 80 (2002) 76.
[15] C.M. Zetterling, M. Östling, N. Nordell, O. Schön, M. Deschler, Appl. Phys. Lett. 70 (1997) 3549.
[16] C.M. Zetterling, M. Östling, K. Wongchotigul, M.G. Spencer, X. Tang, C.I. Harris, N. Nordell, S.S. Wong, J. Appl. Phys. 82 (1997) 2990.
[17] Z. Feng, C. Yu, J. Li, Q. Liu, Z. He, X. Song, J. Wang, S. Cai, Carbon 75 (2014) 249.
[18] A. Badmaev, Y. Che, Z. Li, C. Wang, C. Zhou, ACS Nano 6 (2012) 3371.
[19] M. Avice, U. Grossner, I. Pintilie, B.G. Svensson, M. Servidori, R. Nipoti, O. Nilsen, H. Fjellvag, J. Appl. Phys. 102 (2007) 054513.
[20] S.S. Suvanam, M. Usman, D. Martin, M.G. Yazdi, M. Linnarsson, A. Tempez, M. Götelid, A. Hallén, Appl. Surf. Sci. 433 (2018) 108.
[21] M. Usman, S.S. Suvanam, M.K. Linnarsson, A. Hallén, Mater. Sci. Semicond. Process. 81 (2018) 118.
[22] H. Yoshioka, M. Yamazaki, S. Harada, AIP Adv. 6 (2016) 105206.
[23] T. Hatayama, S. Hino, N. Miura, T. Oomori, E. Tokumitsu, IEEE Trans. Electron Devices 55 (2008) 2041.
[24] J.T. Chen, J.W. Pomeroy, N. Rorsman, C. Xia, C. Virojanadara, U. Forsberg, M. Kuball, E. Janzén, J. Cryst. Growth 428 (2015) 54.
[25] R.Y. Khosa, E.B. Thorsteinsson, M. Winters, N. Rorsman, R. Karhu, J. Hassan, E.Ö. Sveinbjörnsson, AIP Adv. 8 (2018) 025304.
[26] F. Allerstam, G. Gudjonsson, H.Ö. Ólafsson, E.Ö. Sveinbjörnsson, T. Rödle, R. Jos, Semicond. Sci. Technol. 22 (2007) 307.
[27] E.H. Nicollian, J.R. Brews, MIS (Metal Oxide Semiconductor) Physics and Technology, John Wiley & Sons, New York, USA, 1982.
[28] J.A. Cooper Jr., Phys. Status Solidi 162 (1997) 305.
[29] M. Sadeghi, O. Engström, Microelectron. Eng. 36 (1997) 183.
[30] S. Berberich, P. Godignon, M.L. Locatelli, J. Millán, H.L. Hartnagel, Solid-State Electron. 42 (1998) 915.
[31] L. Gordon, J.L. Lyons, A. Janotti, C.G. Van de Walle, Phys. Rev. B 89 (2014) 085204.
[32] L.X. Yu, W.Y. Yu, P.Z. Yang, L.C. Zhan, W. Jia, B. Yun, T.Y. Dan, L.K. An, S.H. Jun, Chin. Phys. B 24 (2015) 087304.